



**HAL**  
open science

# Revealing the Dynamic Structure of Complex Solid Catalysts Using Modulated Excitation X-ray Diffraction

Davide Ferri, Mark Newton, Marco Di michiel, Gian Luca Chiarello, Songhak Yoon, Ye Lu, Jérôme Andrieux

► **To cite this version:**

Davide Ferri, Mark Newton, Marco Di michiel, Gian Luca Chiarello, Songhak Yoon, et al.. Revealing the Dynamic Structure of Complex Solid Catalysts Using Modulated Excitation X-ray Diffraction. *Angewandte Chemie International Edition*, 2014, 53 (34), pp.8890-8894. 10.1002/anie.201403094 . hal-02326200

**HAL Id: hal-02326200**

**<https://hal.science/hal-02326200>**

Submitted on 6 Sep 2021

**HAL** is a multi-disciplinary open access archive for the deposit and dissemination of scientific research documents, whether they are published or not. The documents may come from teaching and research institutions in France or abroad, or from public or private research centers.

L'archive ouverte pluridisciplinaire **HAL**, est destinée au dépôt et à la diffusion de documents scientifiques de niveau recherche, publiés ou non, émanant des établissements d'enseignement et de recherche français ou étrangers, des laboratoires publics ou privés.

# Seeing further into the dynamic structure of complex solid catalysts using modulated excitation X-ray diffraction\*\*

Davide Ferri,<sup>\*</sup> Mark A. Newton,<sup>\*</sup> Marco Di Michiel,<sup>\*</sup> Gian Luca Chiarello,<sup>§</sup> Songhak Yoon, Ye Lu, Jérôme Andrieux<sup>†</sup>

\* Dr. D. Ferri  
Paul Scherrer Institut, CH-5232 Villigen PSI, Switzerland  
e-mail: davide.ferri@psi.ch

\* Dr. Gian Luca Chiarello, Dr. S. Yoon, Dr. Y. Lu  
Empa, Swiss Federal Laboratories for Materials Science and Technology, Laboratory for Solid State Chemistry and Catalysis, Ueberlandstrasse 129, CH-8600 Dübendorf, Switzerland

\* Dr. M.A. Newton, Dr. M. Di Michiel, Dr. J. Andrieux  
ESRF, 6 Rue Jules Horowitz, F-38043 Grenoble, France  
e-mail: mark.newton@esrf.fr  
e-mail: dimichie@esrf.fr

§ present address: Dipartimento di Chimica, Università degli Studi di Milano, Via C. Golgi 19, I-20133 Milano, Italy

† present address: Université de Lyon, 43 Bd du 11 Nov. 1918, F-69622 Villeurbanne, France

\*\* This work was supported by the Competence Centre for Materials Science and Technology (CCMX) and the Swiss National Science Foundation (SNF) under project Nr. 200021-138068. The authors are grateful to ESRF for beam time allocation at beamlines ID15B and BM23, to Umicore for kindly providing catalyst samples and to Dr. S.K. Matam and Dr. D. Zurita for help during beamtime.

**Abstract:** X-ray diffraction (XRD) is typically silent towards information on low loadings of precious metals on solid catalysts because of their finely dispersed nature. When combined with a concentration modulation approach time-resolved high energy XRD is able to provide the detailed red-ox dynamics of Pd nano-particles of ca. 2 nm in 2 wt% Pd/CZ, an otherwise difficult sample for EXAFS because of the presence of Ce. The detailed temporal evolution of the Pd(111) and Ce(111) reflections together with surface information from synchronous DRIFTS measurements reveals that Ce maintains Pd oxidized during a 30 s CO pulse while reduction is detected at the beginning of the 30 s O<sub>2</sub> pulse. Oxygen is likely transferred from Pd to Ce<sup>3+</sup> before the onset of Pd re-oxidation. In this context, adsorbed carbonates appear to be the rate limiting species for re-oxidation.

Establishing, with the highest level of precision, the structure of functional materials and the structural changes that occur whilst they are operating is a considerable research challenge. This key issue spans a vast range of disciplines as it is fundamental to both practical application and our understanding of why materials behave as they do. Approaches based upon X-ray diffraction (XRD)<sup>[1]</sup> and X-ray absorption spectroscopy (XAS)<sup>[2]</sup> as well as advanced microscopy,<sup>[3]</sup> continue to be at the forefront of this endeavour. This task is made even more challenging by the necessity to be able to observe structural changes – which in themselves may be extremely subtle in nature – while materials are functioning (*in situ* or *operando* conditions). Recently, progress has started to be made in utilizing approaches founded on the basis of lock in amplification to greatly enhance the sensitivity of advanced probes (e.g. infrared<sup>[4]</sup> and UV-vis<sup>[5]</sup> spectroscopies, XAS<sup>[6]</sup> and XRD<sup>[7]</sup>) and therefore resolve aspects of materials behaviour that would otherwise remain extremely difficult or even impossible to observe using conventional analytical approaches.

Synchrotron high energy X-ray diffraction (XRD) can provide adequate time resolution to follow kinetic processes on sub second timescales.<sup>[8]</sup> This approach can permit insights into the behaviour of a support material, promoter phases and, in the case of the heterogeneous catalysts we consider here, the catalytically active precious metal phase, in a single shot. However, for many catalyst formulations XRD is of reduced utility due to the low levels of structural order, domain sizes that are often limited to the sub ca. 5 nm length scales, and complex multiphase patterns that are extremely difficult to disentangle to yield the desired structural precision.<sup>[9]</sup> Practically, only the response of the catalyst support can be often recorded unless larger precious metal particles/oxide phases are present. This detection limit issue may be circumvented by increasing for example the metal loading in order to capture the dynamics of the precious metal active phase,<sup>[10]</sup> however, in doing this the advantage of studying technical catalysts working under representative conditions is lost.

Here, we demonstrate how a modulation approach coupled to phase sensitive detection (PSD)<sup>[4a, 11]</sup> can be applied to a working catalyst using time-resolved high energy X-ray diffraction in combination with X-ray absorption spectroscopy, infrared spectroscopy and mass spectrometry, to observe and start to quantify aspects of the synergetic behaviour between low loaded (ca. 2 wt%) nanoscale Pd<sup>0</sup>/Pd<sup>II</sup> entities and a ceria-zirconia (CZ) support/promoter material. We have chosen a ceria based catalyst because of its extremely wide use in catalysis.<sup>[12]</sup> Ceria is a crucial component of three-way catalysts for automotive pollution control operating under fast periodic red-ox feedstock fluctuations.<sup>[12a]</sup> The Ce<sup>4+</sup>/Ce<sup>3+</sup> red-ox

pair directs the buffering of oxygen during the short fuel rich periods of operation; a function that is absolutely central to the maintenance of efficient catalytic operation. The interface that is achieved through contact of the metal nano-particles with ceria, together with the availability of oxygen under fuel rich conditions, curtails catalyst deactivation and specifically promotes or retards more fundamental aspects of the chemistry occurring on the metallic component compared to the corresponding alumina-based catalysts.<sup>[13]</sup> The nature of the Pd/CZ system, in terms of the low levels and small size of the Pd component, together with the highly absorbing/scattering nature of ceria itself has made detailed understanding of the structure-function relationships and the kinetics of the processes that define its superior behavior, extremely difficult to obtain. We show that by using X-ray diffraction in tandem with the modulation approach and PSD we can go considerably beyond what has been previously attained in related systems<sup>[13b]</sup> in terms of being able to follow some extremely subtle structure-reactive changes that are at the very heart of the superior applied behaviour of difficult materials.

Figure 1(a) shows the colour map representation of a CO/O<sub>2</sub> concentration modulation experiment carried out on 2.2 wt% Pd/CZ at 573 K, where the concentration of CO and O<sub>2</sub> in He is periodically and alternately switched on and off (between 0 and 1 vol%) every 25 s. The sample (67 m<sup>2</sup>/g; 85% Pd dispersion)<sup>[14]</sup> is characterized by a very well dispersed Pd-O phase as demonstrated by the analysis of the local environment around Pd using extended X-ray absorption fine structure (EXAFS, Figure S1); we note that this phase is extremely challenging to observe by electron microscopy methods (Figure S2).<sup>[14]</sup> The time-resolved XRD data of Figure 1(b) present virtually no visible change, except for extremely faint variation of the reflections of cubic CZ. As expected, no reflection of a Pd-containing phase is detectable using common XRD software.

The subtle changes induced by the repeated CO/O<sub>2</sub> pulsing are greatly enhanced by PSD. The set of phase-resolved XRD data (Figure 1(c)) shows a subset of reflections of very low intensity that can now be readily discerned and associated with the temporal response of CZ. Their differential profile reflects a reversible shift of the CZ d spacing according to the environment being experienced. This is indicative of a reversible lattice contraction/expansion as a consequence of oxygen removal and re-insertion, respectively.<sup>[13b]</sup> We note that the amplitude of change now visible is some 60 times less than the intensity of the Bragg reflections observed in the time-resolved data set.

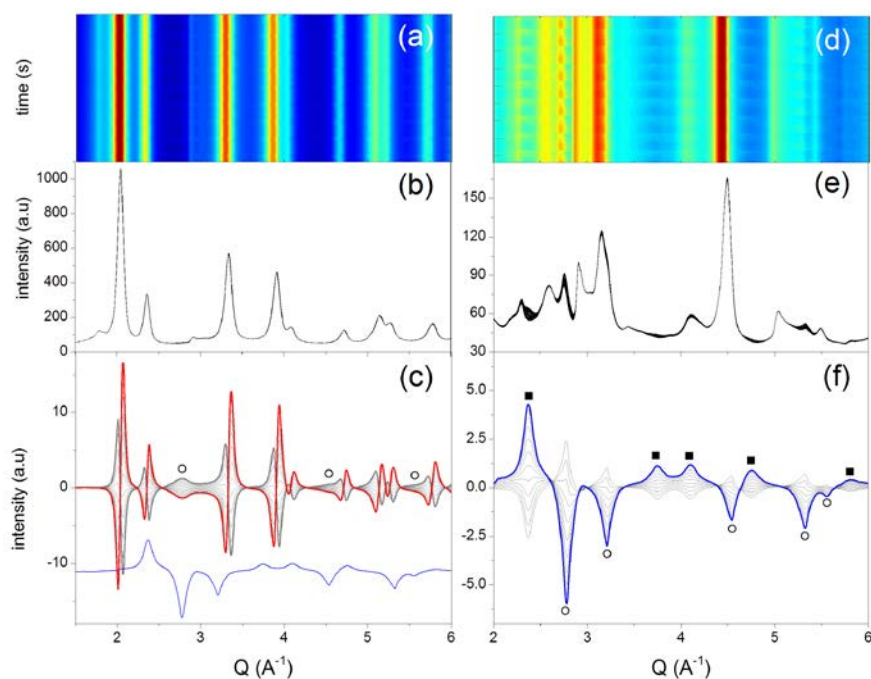


**Figure 1.** (a) Colour map representation and (b) time-resolved hard-XRD patterns of 2 wt% Pd/CZ during a full CO/O<sub>2</sub> modulation experiment at 573 K ( $T = 50$  s). (c) Corresponding set of phase-resolved data. The red profile is the in-phase pattern. Phase-resolved data are shown for the 10-150°  $\phi^{\text{PSD}}$  range. The blue profile is the in-phase pattern obtained for Pd/Al<sub>2</sub>O<sub>3</sub>. (d-f) High energy-XRD data for an identical experiment performed on 2 wt% Pd/Al<sub>2</sub>O<sub>3</sub>. Phase-resolved data are shown for the 70-180°  $\phi^{\text{PSD}}$  range. Pd and PdO reflections are labelled with ○ and ■, respectively.

More importantly, in the current context, a second subset of reflections also appears which are completely invisible in the raw XRD data. The signal at  $2.78 \text{ \AA}^{-1}$  that experiences only an intensity variation is not characteristic of CZ. Further inspection of the PSD data reveals that the signal is accompanied by a series of further features at ca. 3.2, 4.5, 5.3 and  $5.6 \text{ \AA}^{-1}$  that overlap with the CZ reflections. Comparison with the JCPDS reference cards confirms that the set of signals corresponds to metallic Pd ((111), (200), (220), (311) and (222), respectively). This is further corroborated by comparison with the PSD data obtained for a relatively simple system, insofar as Pd/Al<sub>2</sub>O<sub>3</sub> can be considered such. In the 2 wt% Pd/Al<sub>2</sub>O<sub>3</sub> (135 m<sup>2</sup>/g; 20% Pd dispersion, 5.6 nm mean particle size)<sup>[6a]</sup> both PdO and metallic Pd phases are clearly detected and already evident in the conventional time-resolved data (Figure 1(d-f)). A such conventional XRD is clearly sufficient to access detailed structural-reactive kinetics (Figure 1e) of the dominant (Pd/PdO) redox couple in this case. The application of PSD to this case reveals only intensity variations of PdO and Pd reflections. Therefore, in an extremely difficult system for time-resolved spectroscopy such as Pd/CZ the formation of a metallic Pd phase during the CO pulse becomes visible only after application of PSD. The assignment of the reflections at  $2.78 \text{ \AA}^{-1}$  and at higher Q to metallic Pd is further validated by the observation that Pd-free CZ does not exhibit any change in the Q range at 573 K where the Pd phase appears on Pd/CZ (Figure S3). Further, the amplitude of the changes observed for CZ on Pd/CZ is two orders of magnitude more intense than in the absence of Pd, thus clearly demonstrating a pronounced promotion of ceria reduction by Pd induced by the intimate contact of the two phases.<sup>[13b]</sup> However, PSD of the time-resolved data of Pd/CZ fails to provide any evidence of the participation of a PdO phase. Besides the overlap with CZ reflections, the most probable reason for the absence of PdO from PSD is that a defined phase having the structural character of PdO does not form at all in the presence of CZ. This would be consistent with the EXAFS analysis of the as prepared catalyst (Figure S1).

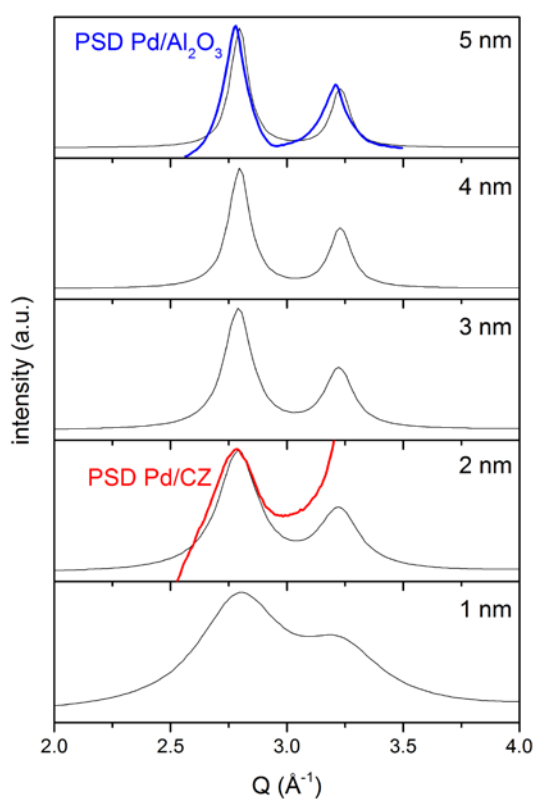


**Figure 2.** Simulated XRD patterns of Pd nano-particles with diameter in the 1-5 nm range in the Pd(111) and Pd(200) region. The red and blue profiles correspond to the in-phase data of Figure 1c (Pd/CZ) and Figure 1f (Pd/Al<sub>2</sub>O<sub>3</sub>), respectively. PSD data are cut for simplicity. The contribution of CZ in the PSD data of Pd/CZ does not allow to detect the Pd(200) reflection.

Based upon the only clearly accessible reflection corresponding to the formation of the metallic Pd phase (Pd(111),  $2.78 \text{ \AA}^{-1}$ ), the estimation of the crystallite size by the Scherrer equation for the PSD data exhibiting the largest amplitude at  $2.78 \text{ \AA}^{-1}$  ( $\phi^{\text{PSD}} = 180^\circ$ ) provides in first approximation a value of 1.9 nm, below the conventional threshold of XRD for this metal loading.<sup>[15]</sup> For the use of the Scherrer formula, it is assumed that strain does not contribute to the observed changes. Conventional strain analysis of the Pd/CZ is hindered because only the Pd(111) reflection is clearly available. The mean particle size of 5.3 nm obtained with the same procedure for a number of reflections of Pd/Al<sub>2</sub>O<sub>3</sub>

corresponding to the PdO and Pd phases is in line with the chemisorption data (see above) and validates the XRD analysis. The simulated diffraction patterns of Pd nano-particles with diameter in the 1-5 nm range (Figure 2) confirmed that the signal observed in the phase-resolved data of Pd/CZ corresponds approximately to 2 nm, which is in striking agreement with the value obtained from the Scherrer equation. Similarly, the width at half height of the in-phase data of Pd/Al<sub>2</sub>O<sub>3</sub> is also very close to that of 5 nm large particles.

The shift of the CZ pattern to low and high Q values upon CO and O<sub>2</sub> pulsing, respectively, that is clearly observed in the PSD data is associated with the partial reduction of Ce<sup>4+</sup> upon introduction of CO. The data shown in Figure 1 indicate that it is not a bulk reduction that is captured under these experimental conditions. Following the approach of Martorana et al.,<sup>[16]</sup> we have determined the fraction of Ce<sup>4+</sup> that has been reduced in the CO pulse. The reliability of the method was confirmed by the measure of the mole content of Ce<sup>4+</sup> (0.54) obtained assuming only a cubic structure for CZ that is compatible with the original CZ composition (Ce<sub>0.6</sub>Zr<sub>0.4</sub>O<sub>2</sub>). The small discrepancy in Ce may lie in a small contribution of the tetragonal phase.<sup>[16]</sup> The very small shift in d spacing (0.11% measured at 573 K (Figure S4)) indicates that only about 6% of Ce<sup>4+</sup> reduces to Ce<sup>3+</sup> (Figure 3a).<sup>[16]</sup> Hence, the observed structural changes are caused by extremely subtle variations of oxygen stoichiometry.

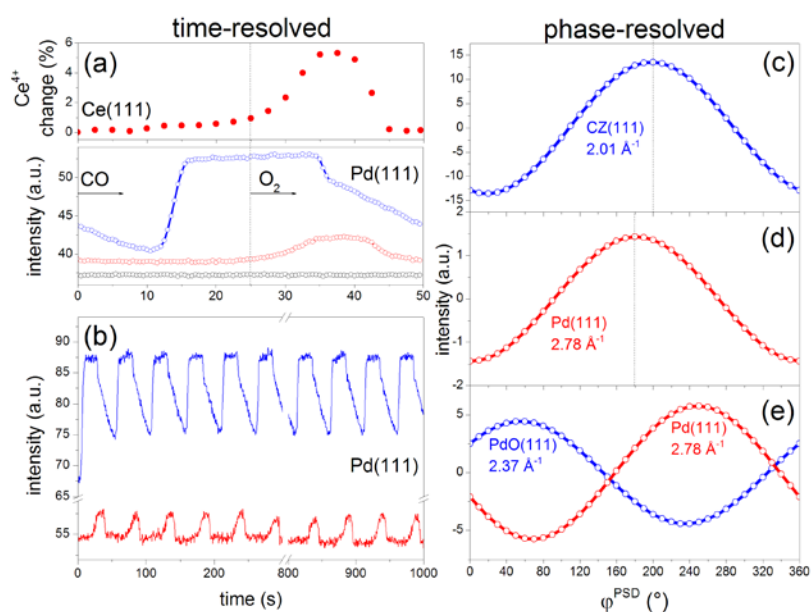


**Figure 3.** Temporal responses of XRD reflections at  $Q = 2.78 \text{ \AA}^{-1}$  (Pd(111)) over (a) one modulation period (averaged data) and (b) the whole CO/O<sub>2</sub> modulation experiment on Pd/CZ (red), Pd/Al<sub>2</sub>O<sub>3</sub> (blue) and CZ (black). The fraction of reduced Ce<sup>4+</sup> over the modulation period is also shown in (a). Right panel: phase angle ( $\phi^{\text{PSD}}$ ) dependence of selected reflections of (c-d) Pd/CZ and (e) Pd/Al<sub>2</sub>O<sub>3</sub>. Vertical bars are used to guide the eye.

The dynamic changes associated with the Pd and CZ reflections identified by PSD can be followed in a temporal manner, thus placing us in a position to extract reduction and re-oxidation kinetics. Figure 3(b) shows that in case of Pd/CZ it is always the same fraction of Pd atoms that responds to the periodic external stimulus, the extent of change remaining constant over the repeated modulation periods. In strong contrast to this behaviour, the Pd(111) reflection of Pd/Al<sub>2</sub>O<sub>3</sub> oscillates around a constant term only after the first CO pulse showing that re-oxidation is not able to completely restore the initial structure of the catalyst, in reason of e.g. particle size effects and the kinetics of re-oxidation. Figure 3(a) also shows the kinetics of the signal at  $2.78 \text{ \AA}^{-1}$  for Pd/CZ and CZ, and for Pd/Al<sub>2</sub>O<sub>3</sub> for comparison, obtained upon averaging over all modulation periods. The temporal profile of the CZ reflections is exemplarily represented by that at  $2.01 \text{ \AA}^{-1}$  and demonstrates the d spacing variation, reflecting the Ce<sup>4+</sup> → Ce<sup>3+</sup> reduction, is synchronous to reduction of Pd<sup>2+</sup>. Detection of the Pd metal phase by XRD is, however, delayed with respect to the point of CO admittance,<sup>[16]</sup> and therefore significantly retarded compared to the earlier reduction of Pd/Al<sub>2</sub>O<sub>3</sub>.

The absence of any XRD response in the CO pulse despite the detection of adsorbed CO in the synchronous DRIFT spectra (Figure S5) indicates that CO consumes the available oxygen provided by ceria within the reduction pulse. This matches the broad gaseous CO<sub>2</sub> profile observed by DRIFTS and MS that encompasses the whole CO pulse (Figure 4c).<sup>[136]</sup> CO oxidation by Pd exploiting oxygen from CZ is not exhausted until the end of the CO pulse. The temporal profiles of Pd/CZ in Figure 3(a,b) and

the CO<sub>2</sub> evolution profiles (Figure 4c) are extremely different from those observed on CZ and Pd/Al<sub>2</sub>O<sub>3</sub> and demonstrate the well-known improvement of stability of Pd<sup>2+</sup> by contact with CZ, and thus improved resistance toward reduction that is offered by the oxygen storage capacity of ceria.

The appearance of the metallic Pd phase on Pd/CZ only at the very end of the CO pulse is delayed compared to the IR observation, suggesting that the reduced Pd atoms do not form a XRD active phase. On the contrary, adsorption of CO on the metal oxide is already detected by XRD by the increase to ca. 1% of Ce<sup>3+</sup> ca. 10 s from admittance of CO. The ordered Pd phase grows in and persists in the O<sub>2</sub> pulse before vanishing synchronously with Ce re-oxidation. Ce<sup>3+</sup> acts as a sink for oxygen and Pd oxidation commences once Ce<sup>3+</sup> has been re-oxidized.

Only the phase angular dependence of the reflections obtained by PSD, for which the temporal profiles are provided in Figure 3, is able to disclose the detail of the kinetics of these processes. Whereas the large phase lag ( $\Delta\phi^{\text{PSD}} = 190^\circ$ ) between PdO (2.37 Å<sup>-1</sup>) and Pd (2.78 Å<sup>-1</sup>) reflections is obvious in Pd/Al<sub>2</sub>O<sub>3</sub> and reflects the conversion of one species into the other (Figure 3e), the small, but measurable only by PSD, phase lag between the reflections of CZ and that of metallic Pd ( $\Delta\phi^{\text{PSD}} = 20^\circ$ ) suggests that metallic Pd<sup>0</sup> evolves (and therefore Pd<sup>2+</sup> reduces) before a change of d spacing of CZ becomes detectable (Figure 3c,d). This is a key observation implying the direct interaction of Pd<sup>2+</sup> and CZ rather than a discrete oxygen transfer process acting between components. The difference becomes more evident by using PSD at higher harmonics where faster processes can be more easily captured but at the expenses of intensity (Figure S6).<sup>[17]</sup> A phase lag of  $\Delta\phi^{\text{PSD}} = 50^\circ$  is observed for  $k = 5$ . This information is not accessible by analysing the raw time-resolved XRD data of Pd/CZ.

The delayed reduction of Pd observed in the high energy XRD data is supported by a similar quick-EXAFS experiment (Figure S7). The levels of Pd<sup>2+</sup> versus Pd(0) present as a function of time obtained from linear combination analysis (LCA, Figure S8) of the Pd K-edge XANES using the bulk PdO and the Pd foil references closely follow the overall temporal behaviour of the Pd(111) reflection. The use of bulk PdO as reference for Pd/CZ is evidently an approximation in this case as a well-defined PdO phase is not detected (from XRD and PSD). Nevertheless, qualitatively the XANES/LCA matches the general behaviour extracted from the XRD. A crucial result is that the reduction of Pd/CZ is considerably retarded compared to the start of the CO pulse and only towards its end is significant Pd reduction observed. Further, the reduced state of Pd/CZ also persists after switching from CO to O<sub>2</sub> as observed in the modulation XRD data. Hence, a striking agreement with respect to the kinetics of Pd reduction-oxidation between XRD and XAS can be demonstrated.

Beside adsorbed CO, readily forming after admittance of CO to both catalysts, a variety of adsorbed carbonate species (1700-1200 cm<sup>-1</sup>) also appear and dominate the IR spectra especially in the case of Pd/CZ (Figure S5). The temporal behaviour of these species, represented by the signal at 1430 cm<sup>-1</sup> (Figure 4), shows that carbonate species are removed much more slowly from the catalysts than CO. After 4 s from the CO→O<sub>2</sub> switch all adsorbed Pd-CO species have disappeared, i.e. much earlier than the disappearance of the metallic Pd phase from the XRD. The removal of adsorbed CO species upon the CO→O<sub>2</sub> switch is fast and matches with the second CO<sub>2</sub> production event in both catalysts. At this point in time when gas phase oxygen is consumed and CO<sub>2</sub> is formed, the reduction of Pd<sup>2+</sup> and ceria becomes XRD (and XAS) visible indicating that oxygen is not yet able to re-oxidise the two components. Oxygen dissociation on Pd followed by spill-over to Ce<sup>3+</sup>, simultaneously to the slower direct dissociation at Ce<sup>3+</sup> defects retards formation of Pd-O bonds (Pd/CZ) or PdO (Pd/Al<sub>2</sub>O<sub>3</sub>). The presence of carbonate-like species in the oxygen pulse seems to correlate with the reduced state of the catalysts indicating that their removal is the limiting step for catalyst (specifically the CZ) re-oxidation.

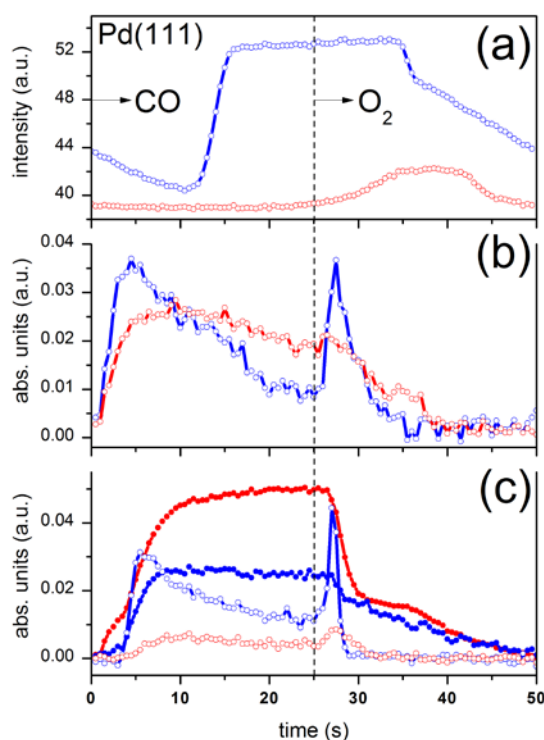


**Figure 4.** DRIFT data during a full CO/O<sub>2</sub> modulation period on Pd/Al<sub>2</sub>O<sub>3</sub> (b) and Pd/CZ (c). CO<sub>2</sub> evolution (2364 cm<sup>-1</sup>); CO<sub>ads</sub>, the difference between CO<sub>B</sub> signals at 1904 cm<sup>-1</sup> and 1927 cm<sup>-1</sup> (1941 cm<sup>-1</sup> in case of Pd/Al<sub>2</sub>O<sub>3</sub>); and, carbonate species observed at ca. 1430 cm<sup>-1</sup> (scaled by factor 5) are shown. For clarity, the top panel (a) shows the data of Figure 3a for the Pd(111) reflection of Pd/CZ and Pd/Al<sub>2</sub>O<sub>3</sub>.

In conclusion, the approach undertaken here provides a vastly superior sensitivity and specificity, toward extremely subtle and perhaps operationally deterministic structural-reactive changes occurring in a complex system working under realistic conditions. Application of phase sensitive detection (PSD) to synchrotron high energy XRD can push the intrinsic detection limits beyond those that are generally accepted. PSD is able to follow the structural changes associated with a subset of the complete material and separates the contribution of two reactively distinct phases (CZ and Pd). The complete kinetic behaviour of small noble metal nano-particles residing upon extremely heavy support materials is typically not readily discernible by microscopic (Z contrast) and diffraction methods (length scales, support contributions) yet becomes accessible in these experiments. The intrinsic advantage of XRD is that it can be used to obtain a global description of a complex catalyst at work, e.g. simultaneously the Pd nano-particles and the spectroscopically difficult metal oxide support. Such enhanced insights should be generically achievable in all situations involving functional materials wherein the reversible cycling (the modulation) of one or more of the intrinsic process variables may be achieved.

**Keywords:** X-ray diffraction, Modulation, Time-resolved, Palladium, Ceria

- [1] J. Hanson, P. Norby, in *In situ characterization of heterogeneous catalysts* (Eds.: J. A. Rodriguez, J. C. Hanson, P. J. Chupas), John Wiley & Sons, **2013**, p. 121.
- [2] S. Bordiga, E. Groppo, G. Agostini, J. A. van Bokhoven, C. Lamberti, *Chem. Rev.* **2013**, *113*, 1736.
- [3] J. C. Yang, M. W. Small, R. V. Grieshaber, R. G. Nuzzo, *Chem. Soc. Rev.* **2012**, *41*, 8179.
- [4] a) D. Baurecht, U. P. Fringeli, *Rev. Sci. Instrum.* **2001**, *72*, 3782; b) T. Bürgi, A. Baiker, *J. Phys. Chem. B* **2002**, *106*, 10649; c) N. Maeda, K. Hungerbühler, A. Baiker, *J. Am. Chem. Soc.* **2011**, *133*, 19567.
- [5] T. Bürgi, *J. Catal.* **2005**, *229*, 55.
- [6] a) D. Ferri, S. K. Matam, R. Wirz, A. Eyssler, O. Korsak, P. Hug, A. Weidenkaff, M. A. Newton, *PCCP* **2010**, *12*, 5634; b) D. Ferri, M. A. Newton, M. Nachtegaal, *Top. Catal.* **2011**, *54*, 1070; c) C. F. J. König, J. A. van Bokhoven, T. J. Schildhauer, M. Nachtegaal, *J. Phys. Chem. C* **2012**, *116*, 19857; d) C. F. J. König, T. J. Schildhauer, M. Nachtegaal, *J. Catal.* **2013**, *305*, 92.
- [7] a) D. Chernyshov, W. van Beek, H. Emerich, M. Milanesio, A. Urakawa, D. Viterbo, L. Palin, R. Caliandro, *Acta Crystall. A* **2011**, *67*, 327; b) W. van Beek, H. Emerich, A. Urakawa, L. Palin, M. Milanesio, R. Caliandro, D. Viterbo, D. Chernyshov, *J. Appl. Crystall.* **2012**, *45*, 738; c) R. Caliandro, D. Chernyshov, H. Emerich, M. Milanesio, L. Palin, A. Urakawa, W. van Beek, D. Viterbo, *J. Appl. Crystall.* **2012**, *45*, 458; d) D. Ferri, M. A. Newton, M. Di Michiel, S. Yoon, G. L. Chiarello, V. Marchionni, S. K. Matam, A. Weideklaff, F. Wen, J. Gieshoff, *PCCP* **2013**, *15*, 8629.
- [8] M. A. Newton, M. Di Michiel, A. Kubacka, M. Fernandez-Garcia, *J. Am. Chem. Soc.* **2010**, *132*, 4540.

- [9] G. Figherazzi, P. Canton, P. Riello, N. Pernicone, F. Pinna, M. Battagliarin, *Langmuir* **2000**, *16*, 4539.
- [10] a) Z. Kaszkur, *J. Appl. Cryst.* **2000**, *33*, 1262; b) J. D. Grunwaldt, N. van Vegten, A. Baiker, *Chem. Commun.* **2007**, 4635; c) F. Hasché, M. Oezaslan, P. Strasser, *ChemPhysChem* **2012**, *13*, 828.
- [11] Phase sensitive detection (PSD):
- $$I_k^{\phi^{PSD}}(e) = \frac{2}{T} \int_0^T I(e, t) \sin(k\omega t + \phi_k^{PSD}) dt$$
- where T is the length of one period,  $\omega$  is the modulation frequency, k is the demodulation index (k= 1),  $\phi_k^{PSD}$  is the demodulation phase angle for  $k\omega$  demodulation and I(t) and  $I_k$  are the responses in the time- and phase-domains, respectively. A more specific equation for modulated excitation X-ray diffraction is to be found in ref. 6c.
- [12] a) A. Trovarelli, Imperial College Press, London, **2002**; b) A. Trovarelli, C. de Leitenburg, M. Boaro, G. Dolcetti, *Catal. Today* **1999**, *50*, 353; c) W. C. Chueh, C. Falter, M. Abbott, D. Scipio, P. Furler, S. M. Haile, A. Steinfeld, *Science* **2010**, *330*, 1797; d) G. Vilé, B. Bridier, J. Wichert, J. Perez-Ramirez, *Angew. Chemie Int. Ed.* **2012**, *51*, 8620.
- [13] a) Y. Nagai, K. Dohmae, Y. Ikeda, N. Takagi, T. Tanabe, N. Hara, G. Gilera, S. Pascarelli, M. A. Newton, O. Kuno, H. Jiang, H. Shinjoh, S. Matsumoto, *Angew. Chemie Int. Ed.* **2008**, *47*, 9303; b) M. A. Newton, M. Di Michiel, A. Kubacka, A. Iglesias-Juez, M. Fernandez-Garcia, *Angew. Chemie Int. Ed.* **2012**, *51*, 2363; c) M. Hatanaka, N. Takahashi, N. Takahashi, T. Tanabe, Y. Nagai, A. Suda, H. Shinjoh, *J. Catal.* **2009**, *266*, 182.
- [14] S. K. Matam, A. Eyssler, P. Hug, N. van Vegten, A. Baiker, A. Weidenkaff, D. Ferri, *Appl. Catal. B: Environmental* **2010**, *94*, 77.
- [15] H. P. Klug, L. E. Alexander, *X-ray diffraction procedure for polycrystalline and amorphous materials*, John Wiley and Sons, New York, **1954**.
- [16] A. Martorana, G. Deganello, A. Longo, F. Deganello, L. Liotta, A. Macaluso, G. Pantaleo, A. Balerna, C. Meneghini, S. Mobilio, *J. Synchrotron Rad.* **2003**, *10*, 177.
- [17] V. Marchionni, M. A. Newton, A. Kambolis, S. K. Matam, A. Weidenkaff, D. Ferri, *Catal. Today*, <http://dx.doi.org/10.1016/j.cattod.2013.10.082>.